As. J. Energy Env. **2007**, 08(01), 490-495

Asian Journal on Energy and Environment

ISSN 1513-4121

Available online at www.asian-energy-journal.info

Electrochemical Property of Cobalt Vanadium Oxide CoV_3O_8 for Lithium Ion Battery

Shin-nosuke Ichikawa*, Mitsuhiro Hibino and Takeshi Yao

Graduate School of Energy Science, Kyoto University, Kyoto, Japan

*Author to whom correspondence should be addressed, email: hin-nosuke@t27a0221.mbox.media.kyoto-u.ac.jp

Abstract: Cobalt vanadium oxide CoV_3O_8 possessing tunnel space along the c axis in the crystal structure was synthesized by a solid state reaction and structurally analyzed by the Rietveld method. The electrochemical lithium insertion-extraction and cycle properties were investigated. CoV_3O_8 exhibited different electrochemical behaviors between the first cycle and the later. This oxide showed discharge profile with small potential change in the first discharge process, in which amorphous phase may be generated by lithium insertion into CoV_3O_8 from XRD measurement. In contrast, relatively large potential change was observed in discharge-charge profile of the second cycle or later. Lithium may be inserted into and extracted from the amorphous phase generated during the first discharge process. As a result, the sample showed reversible lithium insertion and good cycle performance after the second cycle.

Keywords: Cobalt Vanadium Oxide, CoV_3O_8, Solid-state Reaction, Lithium Ion Battery, Cathode Material

Introduction

Transition metal oxides have been extensively studied in terms of electrode materials for lithium ion batteries. Among them, vanadium oxides are one of the most promising materials due to availability, low toxicity [1-3], and low cost. These vanadium oxides, however, are liable to collapse structurally by repetitions of discharge and charge, leading to capacity fade. It is well known that the structure and morphology of vanadium oxide can strongly influence its electrochemical performance [4]. The preparation in the form of nanoparticles [5], xerogels [6-8], or aerogels [9], is one approach for an improvement of such a poor cyclability. The preparation and application of V_2O_5-based composite, such as MO-V_2O_5 (M: Ni, Ti) is another approach to improve the cyclability [10,11]. A vanadium-based complex oxide that has intercalation sites and conduction paths of lithium ion is also one of

candidates. Previously, hydrothermal synthesis and the structure of a cobalt vanadium oxide CoV_3O_8 have been reported by Y. Oka et al. [12]. The CoV_3O_8 has tunnel space along the c-axis in the crystal structure (Fig. 1) and is expected to have good electrochemical performance. However, hydrothermal method allows us to obtain only a small amount of CoV_3O_8 In the present study, we synthesized CoV_3O_8 by solid-state reaction for preparation of enough amount to investigate its electrochemical property. The obtained $CoV_3O_8$was examined as an electrode material for lithium ion battery.

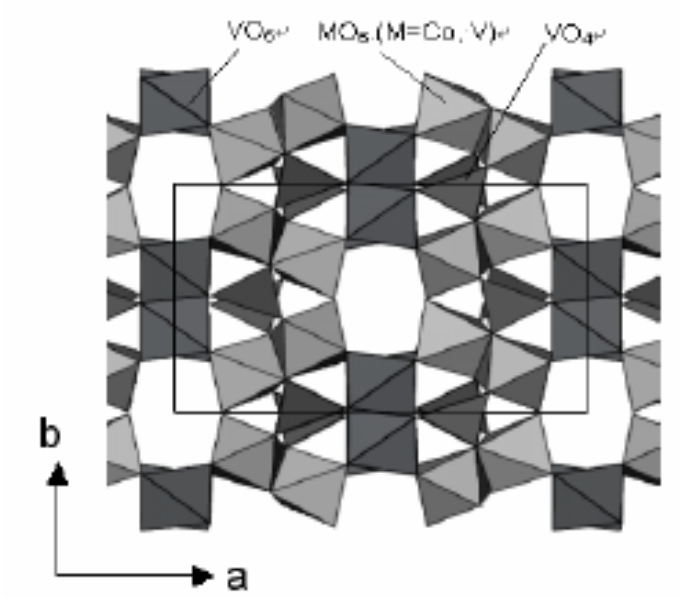

Fig. 1 Polyhedral representation of the crystal structure of CoV_3O_8 projected onto ab plane.

Methodology

Sample preparation

Cobalt oxide CoO, vanadium dioxide V_2O_4 and vanadium pen toxide V_2O_5 were mixed in the molar ratio of Co:V:O = 1:3:8, and pressed cold-is statically into a pellet. The pellet was sealed in a silica tube and heat-treated at 600°C for three days. Then, CoV_3O_8 was obtained.

Electrochemical measurement

Electrochemical measurements were carried out using three-electrode cells. The working electrode consisted of the active material, acetylene black as a conducting additive, poly(tetrafluoro-ethylene) as a binder in the weight ratio 80:15:5 and was pressed on a Ni mesh as a current collector. The counter and reference electrodes were lithium metals. The electrolyte was 1 $mol \cdot dm^{-3}$ $LiClO_4$ dissolved in Ethylene carbonate and 1,2-Dimethoxyethane (1:1 v/v). Cyclic voltammetry was performed between 1.5 and 4.0 V at a scan rate 0.1 $mV \cdot s^{-1}$. Discharge-charge cycle test was carried out between 1.5 and 4.0 V vs. Li^+/Li with constant current density of 80 $mA \cdot g^{-1.}$

X-ray diffraction and Rietveld method

Powder X-ray diffraction (XRD) pattern was taken on the sample. The crystal structure was analyzed by Rietveld method. For the sample after the 21st discharge, the working electrode of electrochemical cell was detached from the cell, placed on a zero background plate of quartz and set in a sealed holder in an argon gas system. This holder was fixed to a diffractometer for XRD measurement.

Results and Discussion

X-ray diffraction and Rietveld method

The result of Rietveld refinement for the CoV_3O_8 sample obtained by solid-state reaction is shown in Fig. 2 [13]. The observed XRD pattern contained 935 reflections. The calculated XRD pattern agreed with the observed one. The reliability indexes were R_{wp} = 0.091, R_B = 0.049, R_F = 0.028, and GOF = 2.77. Considering that a number of peaks were observed and overlapped, in particular at high angles, these result was acceptable. Thus, it was indicated that the CoV_3O_8 obtained by the solid-state reaction has the same crystal structure as that of the hydrothermally synthesized one

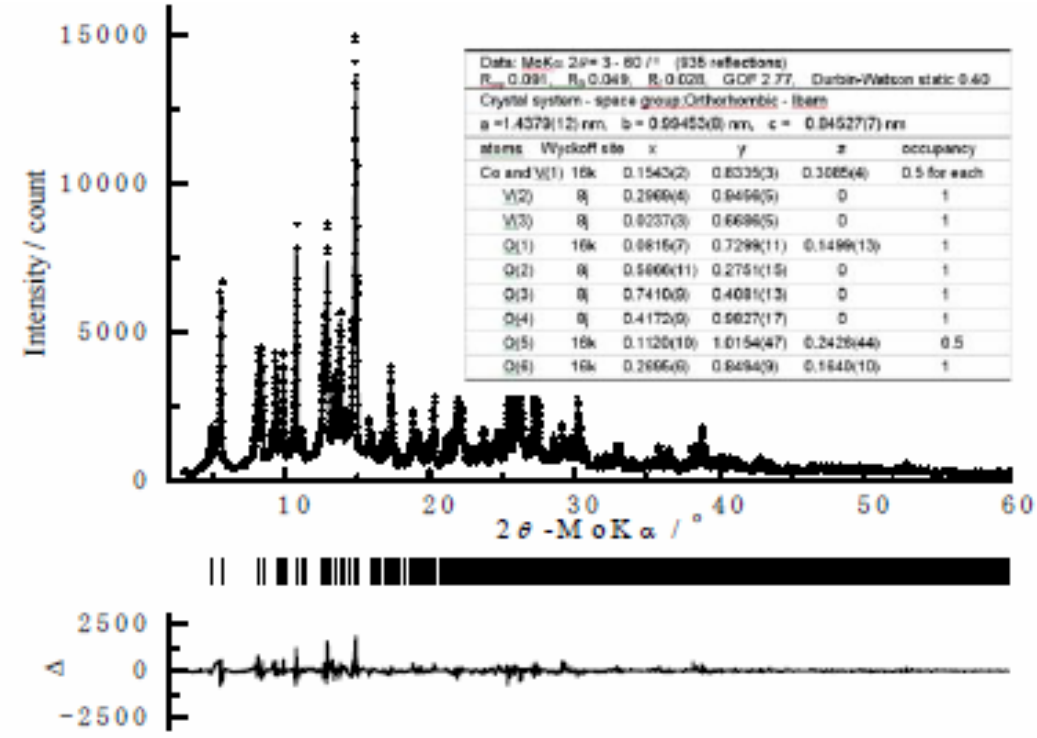

Fig. 2 The result of Rietveld analysis for CoV_3O_8 Inserted table shown crystallographic parameter for CoV_3O_8 refined by Rietveld analysis.

Electrochemical measurements

Figure 3 shows a cyclic voltammogram of the CoV_3O_8. In the first cathodic process, three reduction peaks at 2.4, 2.1, and 1.95 V were observed. For the first anodic scan, one broad oxidation peak around 2.7 V appeared. In the second cycle, one broad reduction peak around 2.0 V, which is different from the potentials of the peaks in the first cathodic scan, was observed. In contrast, oxidation behavior in the second cycle is similar to that in the first cycle. These indicate that electrochemical reaction after the second cycle occurred in one-step reversibly.

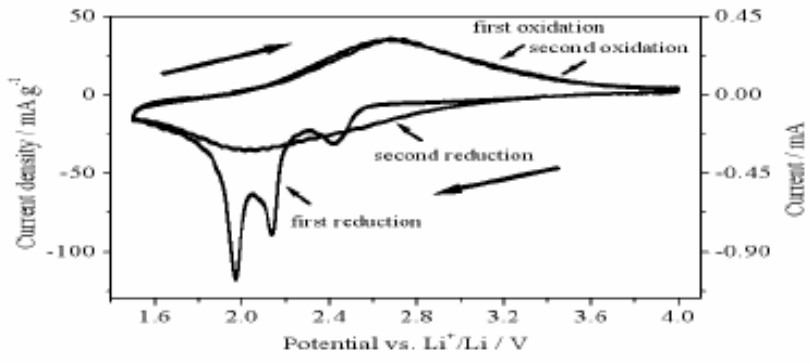

Fig. 3 Cyclic voltammogram of CoV_3O_8

Figure 4 shows discharge-charge curves of CoV_3O_8 at the first, second and 20th cycles, and Fig. 5 shows specific capacity of discharge and charge for CoV_3O_8 as a function of cycle number. In the first discharge, three potential plateaus were observed around 2.4, 2.1 and 1.95 V. In the first charge, the potential was distributed around 2.7 V. In the second and later discharge-charge cycles, electrochemical reaction proceeded in one-step. These results corresponded to the above cyclic voltammetric observation. After the second cycle, integration of cathodic current almost matched that of anodic current. It indicates that lithium reacted electrochemically with the sample reversibly. As a result, this material exhibited good discharge-charge cycle performance.

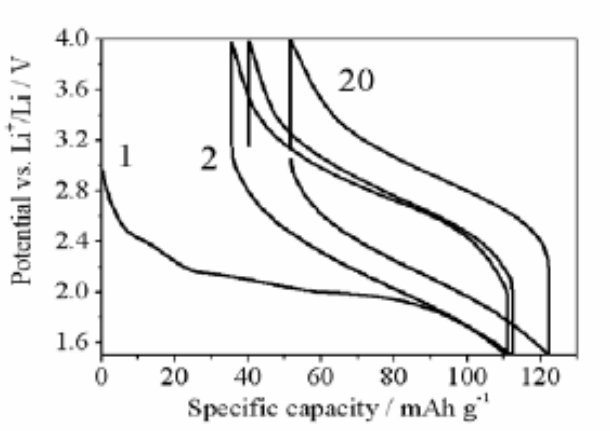

Fig. 4 Discharge-charge curves of CoV_3O_8

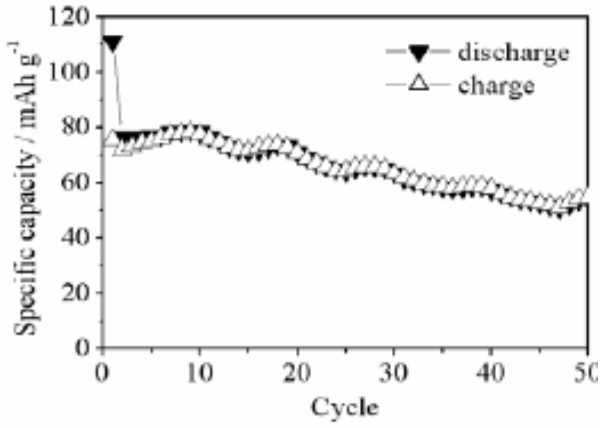

Fig. 5 Specific Capacity of discharge and charge for CoV_3O_8 as a function of cycle number.

X-ray diffraction

Figure 6 shows the XRD profile for the electrode sample after the 21st discharge. The electrode was on a discharged state and lithium ion was left inserted. No peak angles of CoV_3O_8 changed in spite of lithium insertion into the sample. However, the intensity of the peaks of CoV_3O_8 declined while additional unidentified peaks appeared at 44^o and 63.5^o in the profile of the sample after 21^{st} discharge. In the electrochemical measurement of CoV_3O_8mentioned above, the sample showed large slope after the second cycle, compared to normal crystalline electrode materials that lithium can be inserted into and extracted from. It implies that the profile of second discharge-charge cycle or later was due to lithium insertion into and extraction from amorphous material which was generated during the first discharge process. The generation of amorphous may be supported by the fact that the intensity of the peaks of CoV_3O_8 decreased and the halo around 30^o in the XRD profile of the sample after 21st discharge appeared (see an inserted figure in Fig. 5). Good reversibility may be responsible for the newly generated amorphous phase due to its structural flexibility with respect to lithium insertion and extraction. Though lithium was reversibly inserted into the amorphous phase, the contact condition between the amorphous material and acetylene black must be unfavorable, leading to capacity decrease. In this study, since CoV_3O_8 had partly changed into the amorphous phase, not fully yet, the production of amorphous phase proceeded during repeated discharges. That could be one of main causes of gradual reduction of capacity by cycle repetition

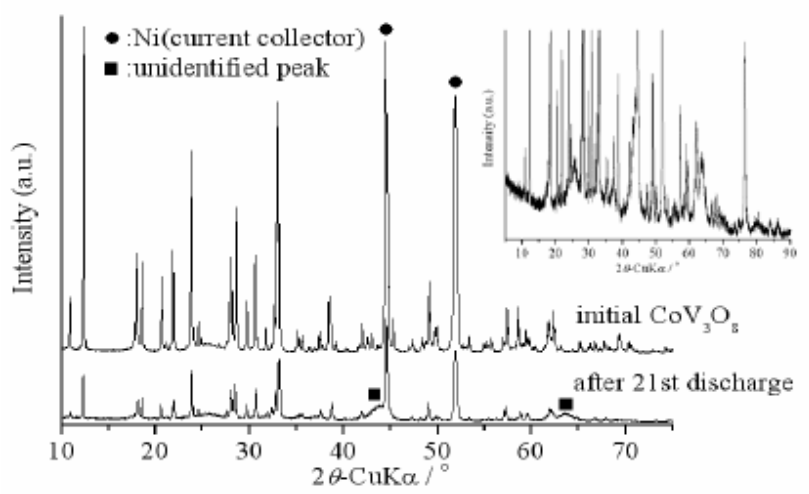

Fig. 6 XRD profiles of the sample after 21 at discharge and the initial CoV_3O_8 as a reference Inserted figure show the profile of the former sample

Conclusion

CoV_3O_8, which has tunnel space along the c axis in the crystal structure, was synthesized by solid-state reaction. Both cyclic voltammetry and multicycle discharge-charge measurement indicated that lithium was inserted into and extracted from the sample reversibly after the second cycle and that the sample exhibited good discharge-charge cycle performance. For the first lithium insertion into CoV_3O_8, the crystal phase of CoV_3O_8 was changed into amorphous one. The amorphous substance is allowed to discharge and charge reversibly after the second cycle. The good cycle performance of CoV_3O_8 may be caused by lithium insertion into and extraction from the generated amorphous because the structure of amorphous can be flexible with respect to lithium insertion and extraction. We concluded that CoV_3O_8 is promising for an electrode material of lithium ion battery.

References

[1] J.M. Cocciantelli, J. P. Doumerc, M. Pouchard, M. Broussely and J. Labat, (1991) *J. Power Sources*, **34**, (2), pp. 103-111.

[2] J. M. Cocciantelli, M. Menetrier, C.Delmas, J. P. Doumerc, M. Pouchard and P. Hagenmuller, (1992) *Solid State Ionics*, **50**, (1-2), pp. 99-105.

[3] C. Delmas, H. Cognac-Auradou, J. M. Cocciantelli, M. Menetrier, and J. P. Doumerc, (1994), *Solid State Ionics*, **69**, (3-4), pp. 257-264.

[4] J. Livage, (1991) *Chem. Mater*., **3**, (4), pp. 578-593.

[5] A.M. Kannan, A. Manthiram, (2003) *Solid State Ionics*, **159**, (3-4), pp. 265-271.

[6] R. Baddour, J.P. Pereira-Ramos, R. Messina and J. Perichon, (1990) *J. Electroanal. Chem.*, **277**, (1-2), pp. 359-366.

[7] F. Coustier, J. Hill, B. B. Owens, S. Passerini, W. H. Smyrl, (1999) *J. Electrochem. Soc.*, **146**, (4), pp. 1355-1360.

[8] T. Kudo, Y. Ikeda, T. Watanabe, M. Hibino, M. Miyayama, H. Abe, K. Kajita, (2002) *Solid State Ionics*, **152**, pp. 833-841.

[9] G. Sudant, E. Baudrin, B. Dunn, J. M. Tarascon, (2004) *J. Electrochem. Soc*., **151**, (5), pp. A666-A671.

[10] E. Andrukaitis, (2003) *J. Power Sources*, **119**, pp. 205-210.

[11] Hai-Rong Liu, Yan-Qiu Chu, Zheng-Wen Fu, Qi-Zong Qin, (2003) *J. Power Sources*, **124**, (1), pp. 163-169.

[12] Y. Oka, T. Yao, N. Yamamoto and Y. Ueda, (1998) *J. Solid State Chem.*, **141**, (1), pp. 133-139.

[13] M. Hibino, N. Ozawa, T. Murakami, M. Nakamura and T. Yao, (2005) *Electrochem. Solid-State Lett.*, **8,** (10), pp. A500-A503.